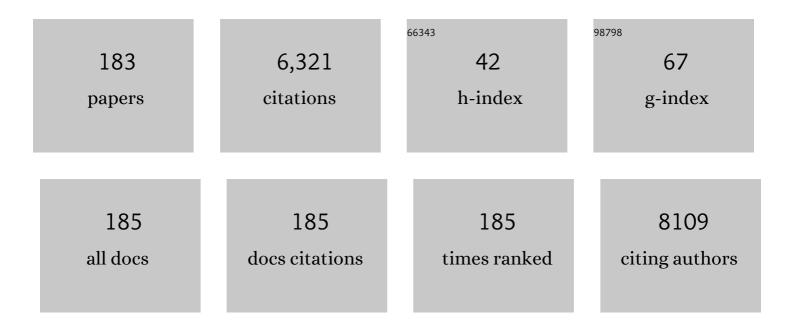
## Dianzeng Jia

List of Publications by Year in descending order

Source: https://exaly.com/author-pdf/2862543/publications.pdf Version: 2024-02-01



#	Article	IF	CITATIONS
1	Inâ€situ expansion strategy towards hierarchical mesoporousÂcarbon: Formation mechanism and applicationÂin supercapacitors. International Journal of Energy Research, 2022, 46, 7249-7260.	4.5	13
2	Designed Formation of Yolk–Shell-Like N-Doped Carbon-Coated Si Nanoparticles by a Facile Method for Lithium-Ion Battery Anodes. ACS Applied Energy Materials, 2022, 5, 1471-1477.	5.1	14
3	A graphdiyne oxide composite membrane for active electrolyte enhanced supercapacitors with super long self-discharge time. Journal of Materials Chemistry C, 2022, 10, 2821-2827.	5.5	12
4	Solar-driven simultaneous desalination and power generation enabled by graphene oxide nanoribbon papers. Journal of Materials Chemistry A, 2022, 10, 9184-9194.	10.3	17
5	Improving the surface area of metal organic framework-derived porous carbon through constructing inner support by compatible graphene quantum dots. Journal of Colloid and Interface Science, 2022, 623, 77-85.	9.4	22
6	Coaxial spinning fabricated high nitrogen-doped porous carbon walnut anchored on carbon fibers as anodic material with boosted lithium storage performance. Journal of Colloid and Interface Science, 2021, 586, 371-380.	9.4	13
7	Restraining polysulfide shuttling by designing a dual adsorption structure of bismuth encapsulated into carbon nanotube cavity. Nanoscale, 2021, 13, 10320-10328.	5.6	4
8	Simple synthesis and electrochemical performance of <scp> NaVSi <sub>2</sub> O <sub>6</sub> </scp> as a new sodiumâ€ion cathode material. International Journal of Energy Research, 2021, 45, 10746-10751.	4.5	4
9	A dualâ€activation strategy to tailor the hierarchical porous structure of biomassâ€derived carbon for ultrahigh rate supercapacitor. International Journal of Energy Research, 2021, 45, 9284-9294.	4.5	15
10	A Novel Carbon Support: Few‣ayered Graphdiyneâ€Decorated Carbon Nanotubes Capture Metal Clusters as Effective Metalâ€Supported Catalysts. Small, 2021, 17, e2006442.	10.0	32
11	Saccharin Anion Acts as a "Traffic Assistant―of Zn <sup>2+</sup> to Achieve a Long-Life and Dendritic-Free Zinc Plate Anode. ACS Applied Materials & Interfaces, 2021, 13, 29631-29640.	8.0	26
12	Carbon nanofiber@ZIF-8 derived carbon nanosheet composites with a core–shell structure boosting capacitive deionization performance. Journal of Materials Chemistry A, 2021, 9, 18604-18613.	10.3	46
13	Ni@Ni <sub>3</sub> N Embedded on Three-Dimensional Carbon Nanosheets for High-Performance Lithium/Sodium–Sulfur Batteries. ACS Applied Materials & Interfaces, 2021, 13, 48536-48545.	8.0	23
14	In situ redox reaction induced firmly anchoring of Na3V2(PO4)2F3 on reduced graphene oxide & carbon nanosheets as cathodes for high stable sodium-ion batteries. Journal of Power Sources, 2021, 516, 230515.	7.8	21
15	Single-Atom Ru on Al <sub>2</sub> O <sub>3</sub> for Highly Active and Selective 1,2-Dichloroethane Catalytic Degradation. ACS Applied Materials & Interfaces, 2021, 13, 53683-53690.	8.0	16
16	NiS nanosheets with novel structure anchored on coal-based carbon fibers prepared by electrospinning for flexible supercapacitors. CrystEngComm, 2020, 22, 1625-1632.	2.6	33
17	Nitrogen, Phosphorus Co-doped Carbon Obtained from Amino Acid Based Resin Xerogel as Efficient Electrode for Supercapacitor. ACS Applied Energy Materials, 2020, 3, 957-969.	5.1	54
18	Ultralight and highly compressible coal oxide-modified graphene aerogels for organic solvent absorption and light-to-heat conversion. New Journal of Chemistry, 2020, 44, 2228-2235.	2.8	10

#	Article	IF	CITATIONS
19	Aggregation-induced emission characteristics of <i>o</i> -carborane-functionalized fluorene and its heteroanalogs: the influence of heteroatoms on photoluminescence. Materials Chemistry Frontiers, 2020, 4, 257-267.	5.9	21
20	High-Performance Gas Sensor of Polyaniline/Carbon Nanotube Composites Promoted by Interface Engineering. Sensors, 2020, 20, 149.	3.8	52
21	Enabling a Large Accessible Surface Area of a Pore-Designed Hydrophilic Carbon Nanofiber Fabric for Ultrahigh Capacitive Deionization. ACS Applied Materials & Interfaces, 2020, 12, 49586-49595.	8.0	32
22	Carbon materials for high mass-loading supercapacitors: filling the gap between new materials and practical applications. Journal of Materials Chemistry A, 2020, 8, 21930-21946.	10.3	94
23	Carbon block anodes with columnar nanopores constructed from amine-functionalized carbon nanosheets for sodium-ion batteries. Journal of Materials Chemistry A, 2020, 8, 24393-24400.	10.3	11
24	Template Construction of Porous CoP/COP <sub>2</sub> Microflowers Threaded with Carbon Nanotubes toward High-Efficiency Oxygen Evolution and Hydrogen Evolution Electrocatalysts. Inorganic Chemistry, 2020, 59, 12232-12239.	4.0	13
25	Coal-based 3D hierarchical porous carbon aerogels for high performance and super-long life supercapacitors. Scientific Reports, 2020, 10, 7022.	3.3	25
26	Boosting the piezocatalytic performance of Bi <sub>2</sub> WO <sub>6</sub> nanosheets towards the degradation of organic pollutants. Materials Chemistry Frontiers, 2020, 4, 2096-2102.	5.9	50
27	Effective promoting piezocatalytic property of zinc oxide for degradation of organic pollutants and insight into piezocatalytic mechanism. Journal of Colloid and Interface Science, 2020, 577, 290-299.	9.4	84
28	Selfâ€Assembly of Perovskite CsPbBr 3 Quantum Dots Driven by a Photoâ€Induced Alkynyl Homocoupling Reaction. Angewandte Chemie, 2020, 132, 17360-17366.	2.0	11
29	Selfâ€Assembly of Perovskite CsPbBr <sub>3</sub> Quantum Dots Driven by a Photoâ€Induced Alkynyl Homocoupling Reaction. Angewandte Chemie - International Edition, 2020, 59, 17207-17213.	13.8	19
30	N/S co-doped coal-based porous carbon spheres as electrode materials for high performance supercapacitors. RSC Advances, 2020, 10, 11033-11038.	3.6	14
31	B/N-Codoped Carbon Nanosheets Derived from the Self-Assembly of Chitosan–Amino Acid Gels for Greatly Improved Supercapacitor Performances. ACS Applied Materials & Interfaces, 2020, 12, 18692-18704.	8.0	98
32	Graphene Quantum Dot Reinforced Electrospun Carbon Nanofiber Fabrics with High Surface Area for Ultrahigh Rate Supercapacitors. ACS Applied Materials & Interfaces, 2020, 12, 11669-11678.	8.0	67
33	Facile strategy for the fabrication of noble metal/ZnS composites with enhanced photocatalytic activities. RSC Advances, 2020, 10, 4455-4463.	3.6	9
34	A solvent-free strategy to realize the substitution of I <sup>â^'</sup> for IO <sub>3</sub> <sup>â^'</sup> in a BiOIO <sub>3</sub> photocatalyst with an opposite charge transfer path. Green Chemistry, 2020, 22, 1424-1431.	9.0	22
35	Dual-nitrogen-source strategy for N-doped graphitic layer-wrapped metal carbide toward efficient oxygen reduction reaction. Journal of Colloid and Interface Science, 2020, 567, 165-170.	9.4	28
36	Synthesis of Airâ€stable 1T Phase of Molybdenum Disulfide for Efficient Electrocatalytic Hydrogen Evolution. ChemCatChem, 2019, 11, 707-714.	3.7	10

#	Article	IF	CITATIONS
37	Facile synthesis of CoxFe1â^'xP microcubes derived from metal-organic frameworks for efficient oxygen evolution reaction. Journal of Colloid and Interface Science, 2019, 554, 202-209.	9.4	15
38	Cu/Cu <sub>2</sub> O/rGO nanocomposites: solid-state self-reduction synthesis and catalytic activity for <i>p</i> -nitrophenol reduction. New Journal of Chemistry, 2019, 43, 12118-12125.	2.8	33
39	Optimized Synthesis of Nitrogen and Phosphorus Dual-Doped Coal-Based Carbon Fiber Supported Pd Catalyst with Enhanced Activities for Formic Acid Electrooxidation. ACS Applied Materials & Interfaces, 2019, 11, 6431-6441.	8.0	32
40	Interstitial N-doped SrSnO <sub>3</sub> perovskite: structural design, modification and photocatalytic degradation of dyes. New Journal of Chemistry, 2019, 43, 10965-10972.	2.8	14
41	Microfluidically mediated atom-transfer radical polymerization. Chemical Communications, 2019, 55, 7554-7557.	4.1	12
42	Electric field induced manipulation of resistive and magnetization switching in Pt/NiFe1.95Cr0.05O4/Pt memory devices. Applied Physics Letters, 2019, 114, .	3.3	19
43	Zn <sub><i>x</i></sub> Co <sub>1–<i>x</i></sub> MoS <sub>3</sub> Microboxes from Metal–Organic Frameworks as Efficient Electrocatalysts for Hydrogen Evolution Reaction. ACS Sustainable Chemistry and Engineering, 2019, 7, 9800-9807.	6.7	11
44	Optimum Balance of Cu <sup>+</sup> and Oxygen Vacancies of CuO <i><sub>x</sub></i> eO <sub>2</sub> Composites for CO Oxidation Based on Thermal Treatment. European Journal of Inorganic Chemistry, 2019, 2019, 1714-1723.	2.0	28
45	Detection of Triacetone Triperoxide (TATP) Precursors with an Array of Sensors Based on MoS2/RGO Composites. Sensors, 2019, 19, 1281.	3.8	30
46	A green approach to prepare hierarchical porous carbon nanofibers from coal for high-performance supercapacitors. RSC Advances, 2019, 9, 6184-6192.	3.6	22
47	Boosting the supercapacitor performance of activated carbon by constructing overall conductive networks using graphene quantum dots. Journal of Materials Chemistry A, 2019, 7, 6021-6027.	10.3	145
48	LiFePO <sub>4</sub> Particles Embedded in Fast Bifunctional Conductor rGO&C@Li <sub>3</sub> V <sub>2</sub> (PO <sub>4</sub> ) <sub>3</sub> Nanosheets as Cathodes for Highâ€Performance Liâ€Ion Hybrid Capacitors. Advanced Functional Materials, 2019, 29, 1807895.	14.9	42
49	Understanding the structural transformation of carbon black from solid spheres to hollow polyhedra during high temperature treatment. RSC Advances, 2019, 9, 29779-29783.	3.6	9
50	Metal-organic framework-derived metal-free highly graphitized nitrogen-doped porous carbon with a hierarchical porous structure as an efficient and stable electrocatalyst for oxygen reduction reaction. Journal of Colloid and Interface Science, 2019, 535, 415-424.	9.4	29
51	Ultrathin Graphdiyne-Wrapped Iron Carbonate Hydroxide Nanosheets toward Efficient Water Splitting. ACS Applied Materials & Interfaces, 2019, 11, 2618-2625.	8.0	73
52	Multifunctional Singleâ€Crystallized Carbonate Hydroxides as Highly Efficient Electrocatalyst for Full Water splitting. Advanced Energy Materials, 2018, 8, 1800175.	19.5	101
53	Facile Controlled Growth of Podetiumâ€Like MnO <sub>2</sub> Crystals and the Catalytic Effect of MnO <sub>2</sub> /Nâ€Doped Graphene on the Oxygen Reduction Reaction. European Journal of Inorganic Chemistry, 2018, 2018, 1315-1321.	2.0	3
54	Coal-Based Hierarchical Porous Carbon Synthesized with a Soluble Salt Self-Assembly-Assisted Method for High Performance Supercapacitors and Li-Ion Batteries. ACS Sustainable Chemistry and Engineering, 2018, 6, 3255-3263.	6.7	80

#	Article	IF	CITATIONS
55	Hollow and Core–Shell Nanostructure Co <sub>3</sub> O <sub>4</sub> Derived from a Metal Formate Framework toward High Catalytic Activity of CO Oxidation. ACS Applied Nano Materials, 2018, 1, 800-806.	5.0	27
56	Controlled Synthesis of a Three-Segment Heterostructure for High-Performance Overall Water Splitting. ACS Applied Materials & Interfaces, 2018, 10, 1771-1780.	8.0	22
57	Rational design of hybrid porous nanotubes with robust structure of ultrafine Li4Ti5O12 nanoparticles embedded in bamboo-like CNTs for superior lithium ion storage. Journal of Materials Chemistry A, 2018, 6, 3342-3349.	10.3	27
58	Enhanced catalytic hydrogenation activity of Ni/reduced graphene oxide nanocomposite prepared by a solid-state method. Journal of Nanoparticle Research, 2018, 20, 1.	1.9	8
59	An effective bifunctional electrocatalysts: Controlled growth of CoFe alloy nanoparticles supported on N-doped carbon nanotubes. Journal of Colloid and Interface Science, 2018, 514, 656-663.	9.4	41
60	Cage carbon-substitute does matter for aggregation-induced emission features of <i>o</i> -carborane-functionalized anthracene triads. Journal of Materials Chemistry C, 2018, 6, 4140-4149.	5.5	49
61	Overall water splitting by graphdiyne-exfoliated and -sandwiched layered double-hydroxide nanosheet arrays. Nature Communications, 2018, 9, 5309.	12.8	287
62	Flexible and Tailorable Naâ^`CO <sub>2</sub> Batteries Based on an Allâ€Solidâ€State Polymer Electrolyte. ChemElectroChem, 2018, 5, 3628-3632.	3.4	42
63	Porous Silicon Photonic Crystals Coated with Ag Nanoparticles as Efficient Substrates for Detecting Trace Explosives Using SERS. Nanomaterials, 2018, 8, 872.	4.1	63
64	Ultramicroporous Carbons Puzzled by Graphene Quantum Dots: Integrated High Gravimetric, Volumetric, and Areal Capacitances for Supercapacitors. Advanced Functional Materials, 2018, 28, 1805898.	14.9	152
65	3D core–shell MoS <sub>2</sub> superspheres composed of oriented nanosheets with quasi molecular superlattices: mimicked embryo formation and Li-storage properties. Journal of Materials Chemistry A, 2018, 6, 18498-18507.	10.3	32
66	An <i>in situ</i> solid-state heredity-restriction strategy to introduce oxygen defects into TiO <sub>2</sub> with enhanced photocatalytic performance. CrystEngComm, 2018, 20, 6156-6164.	2.6	12
67	Molecular Orbital Delocalization/Localization-Induced Crystal-to-Crystal Photochromism of Schiff Bases without <i>ortho</i> -Hydroxyl Groups. Journal of Physical Chemistry C, 2018, 122, 24933-24940.	3.1	4
68	Ni-Doped ZnS Nanospheres Decorated with Au Nanoparticles for Highly Improved Gas Sensor Performance. Sensors, 2018, 18, 2882.	3.8	9
69	Mechanically triggered reversible stepwise tricolor switching and thermochromism of anthracene- <i>o</i> -carborane dyad. Chemical Science, 2018, 9, 5270-5277.	7.4	134
70	V-modified Co <sub>3</sub> O <sub>4</sub> nanorods with superior catalytic activity and thermostability for CO oxidation. CrystEngComm, 2018, 20, 5191-5199.	2.6	24
71	Insights into Crystal Facets of Perovskite SrSnO <sub>3</sub> as Highâ€Performance Photocatalysts toward Environmental Remediation. Chemistry - A European Journal, 2018, 24, 14111-14118.	3.3	21
72	Metal–Organic-Framework-Derived Hollow CoS <sub><i>x</i></sub> @MoS <sub>2</sub> Microcubes as Superior Bifunctional Electrocatalysts for Hydrogen Evolution and Oxygen Evolution Reactions. ACS Sustainable Chemistry and Engineering, 2018, 6, 12961-12968.	6.7	89

#	Article	IF	CITATIONS
73	Structure-Designed Synthesis of CoP Microcubes from Metal–Organic Frameworks with Enhanced Supercapacitor Properties. Inorganic Chemistry, 2018, 57, 10287-10294.	4.0	80
74	In Situ Chelating Synthesis of Hierarchical LiNi <sub>1/3</sub> Co <sub>1/3</sub> Mn <sub>1/3</sub> O <sub>2</sub> Polyhedron Assemblies with Ultralong Cycle Life for Liâ€ion Batteries. Small, 2018, 14, e1704354.	10.0	27
75	Pseudocapacitive Behaviors of Li <sub>2</sub> FeTiO <sub>4</sub> /C Hybrid Porous Nanotubes for Novel Lithium-Ion Battery Anodes with Superior Performances. ACS Applied Materials & Interfaces, 2018, 10, 20225-20230.	8.0	23
76	Solventâ€free Strategy of Photocarriers Accumulated Site and Separated Path for Porous Hollow Spindleâ€ <b>S</b> haped BiPO <sub>4</sub> . ChemCatChem, 2018, 10, 3777-3785.	3.7	12
77	Synthesis, mechanism and efficient modulation of a fluorescence dye by photochromic pyrazolone with energy transfer in the crystalline state. RSC Advances, 2017, 7, 9847-9853.	3.6	5
78	Mn <sub>3</sub> O <sub>4</sub> hollow microcubes and solid nanospheres derived from a metal formate framework for electrochemical capacitor applications. RSC Advances, 2017, 7, 11129-11134.	3.6	24
79	Green solid-state synthesis and photocatalytic hydrogen production activity of anatase TiO <sub>2</sub> nanoplates with super heat-stability. RSC Advances, 2017, 7, 11827-11833.	3.6	25
80	Decoration of Silica Nanoparticles on Polypropylene Separator for Lithium–Sulfur Batteries. ACS Applied Materials & Interfaces, 2017, 9, 7499-7504.	8.0	129
81	A series of new mixed-ligand complexes based on 3,6-bis(imidazol-1-yl)pyridazine: syntheses, structures, and catalytic activities. CrystEngComm, 2017, 19, 3124-3137.	2.6	48
82	Dahlia-shaped BiOCl x I 1â^'x structures prepared by a facile solid-state method: Evidence and mechanism of improved photocatalytic degradation of rhodamine B dye. Journal of Colloid and Interface Science, 2017, 503, 115-123.	9.4	56
83	Solvent-Free Chemical Approach to Synthesize Various Morphological Co <sub>3</sub> O <sub>4</sub> for CO Oxidation. ACS Applied Materials & Interfaces, 2017, 9, 16128-16137.	8.0	136
84	Sandwich-Like CNT@Fe <sub>3</sub> O <sub>4</sub> @C Coaxial Nanocables with Enhanced Lithium-Storage Capability. ACS Applied Materials & Interfaces, 2017, 9, 1453-1458.	8.0	38
85	Hybrid porous bamboo-like CNTs embedding ultrasmall LiCrTiO <sub>4</sub> nanoparticles as high rate and long life anode materials for lithium ion batteries. Chemical Communications, 2017, 53, 1033-1036.	4.1	25
86	In situ solid-state fabrication of hybrid AgCl/AgI/AgIO3 with improved UV-to-visible photocatalytic performance. Scientific Reports, 2017, 7, 12365.	3.3	15
87	Improved rate capability and cycling stability of bicontinuous hierarchical mesoporous LiFePO <sub>4</sub> /C microbelts for lithium-ion batteries. New Journal of Chemistry, 2017, 41, 12969-12975.	2.8	7
88	Hierarchical porous carbon spheres constructed from coal as electrode materials for high performance supercapacitors. RSC Advances, 2017, 7, 45363-45368.	3.6	24
89	Cost-effective synthesis of bamboo-structure carbon nanotubes from coal for reversible lithium storage. RSC Advances, 2017, 7, 34770-34775.	3.6	37
90	High-performance supercapacitors based on conductive graphene combined with Ni(OH) <sub>2</sub> nanoflakes. RSC Advances, 2017, 7, 36617-36622.	3.6	25

#	Article	IF	CITATIONS
91	Solid-state photochromic behavior of pyrazolone 4-phenylthiosemicarbazones. New Journal of Chemistry, 2017, 41, 15229-15235.	2.8	2
92	Facile synthesis of Mn3O4-rGO hybrid materials for the high-performance electrocatalytic reduction of oxygen. Journal of Colloid and Interface Science, 2017, 488, 251-257.	9.4	36
93	Heteroatom-doped graphene as electrocatalysts for air cathodes. Materials Horizons, 2017, 4, 7-19.	12.2	142
94	Synthesis and improved photochromic properties of pyrazolones in the solid state by incorporation of halogen. Spectrochimica Acta - Part A: Molecular and Biomolecular Spectroscopy, 2017, 171, 149-154.	3.9	8
95	The Energy Transfer and Thermal Stability of a Blueâ€Green Color Tunable K <sub>2</sub> CaP <sub>2</sub> O <sub>7</sub> :Ce <sup>3+</sup> ,Tb <sup>3+</sup> Phosphor. Journal of the American Ceramic Society, 2017, 100, 185-192.	3.8	26
96	Hierarchical Mn2O3 Microspheres In-Situ Coated with Carbon for Supercapacitors with Highly Enhanced Performances. Nanomaterials, 2017, 7, 409.	4.1	13
97	Multichannel Discriminative Detection of Explosive Vapors with an Array of Nanofibrous Membranes Loaded with Quantum Dots. Sensors, 2017, 17, 2676.	3.8	12
98	Direct Coal Liquefaction with Fe3O4 Nanocatalysts Prepared by a Simple Solid-State Method. Energies, 2017, 10, 886.	3.1	6
99	Low-temperature CO oxidation over CeO <sub>2</sub> and CeO <sub>2</sub> @Co <sub>3</sub> O <sub>4</sub> core–shell microspheres. New Journal of Chemistry, 2017, 41, 13418-13424.	2.8	49
100	Nitrogenâ€Doped Hollow Amorphous Carbon Spheres@Graphitic Shells Derived from Pitch: New Structure Leads to Robust Lithium Storage. Chemistry - A European Journal, 2016, 22, 2339-2344.	3.3	27
101	High-Performance Manganese Nanoparticles on Reduced Graphene Oxide for Oxygen Reduction Reaction. Catalysis Letters, 2016, 146, 1019-1026.	2.6	22
102	Super high-rate, long cycle life of europium-modified, carbon-coated, hierarchical mesoporous lithium-titanate anode materials for lithium ion batteries. Journal of Materials Chemistry A, 2016, 4, 9949-9957.	10.3	86
103	Facile solid-state synthesis of Fe/FeOOH hierarchical nanostructures assembled from ultrathin nanosheets and their application in water treatment. CrystEngComm, 2016, 18, 8465-8471.	2.6	6
104	Two-dimensional dysprosium-modified bamboo-slip-like lithium titanate with high-rate capability and long cycle life for lithium-ion batteries. Journal of Materials Chemistry A, 2016, 4, 17782-17790.	10.3	35
105	Simple in situ synthesis of carbon-supported and nanosheet-assembled vanadium oxide for ultra-high rate anode and cathode materials of lithium ion batteries. Journal of Materials Chemistry A, 2016, 4, 13907-13915.	10.3	49
106	Interlayer expanded MoS 2 enabled by edge effect of graphene nanoribbons for high performance lithium and sodium ion batteries. Carbon, 2016, 109, 461-471.	10.3	114
107	Self-assembled sulfur/reduced graphene oxide nanoribbon paper as a free-standing electrode for high performance lithium–sulfur batteries. Chemical Communications, 2016, 52, 12825-12828.	4.1	39
108	Design and synthesis of reversible solid-state photochromic pyrazolones by introducing a pyridine ring. Photochemical and Photobiological Sciences, 2016, 15, 1222-1226.	2.9	2

#	Article	IF	CITATIONS
109	Superior Cycle Stability Performance of Quasi-Cuboidal CoV <sub>2</sub> O <sub>6</sub> Microstructures as Electrode Material for Supercapacitors. ACS Applied Materials & Interfaces, 2016, 8, 27291-27297.	8.0	79
110	Zinc and cadmium complexes based on bis-(1H-tetrazol-5-ylmethyl/ylethyl)-amine ligands: structures and photoluminescence properties. CrystEngComm, 2016, 18, 6708-6723.	2.6	30
111	Anatase/rutile titania anchored carbon nanotube porous nanocomposites as superior anodes for lithium ion batteries. CrystEngComm, 2016, 18, 4489-4494.	2.6	17
112	Green synthesis of BiOBr modified Bi <sub>2</sub> O <sub>2</sub> CO <sub>3</sub> nanocomposites with enhanced visible-responsive photocatalytic properties. RSC Advances, 2016, 6, 106046-106053.	3.6	23
113	Luminescence, energy transfer and tunable color of Ce <sup>3+</sup> ,Dy <sup>3+</sup> /Tb <sup>3+</sup> doped BaZn <sub>2</sub> (PO <sub>4</sub> ) <sub>2</sub> phosphors. New Journal of Chemistry, 2016, 40, 3086-3093.	2.8	44
114	Improved electrochemical performance of lithium iron phosphate in situ coated with hierarchical porous nitrogen-doped graphene-like membrane. Journal of Power Sources, 2016, 305, 122-127.	7.8	34
115	Coal based magnetic activated carbon as a high performance adsorbent for methylene blue. Journal of Porous Materials, 2016, 23, 877-884.	2.6	23
116	Porous CNT@Li <sub>4</sub> Ti <sub>5</sub> O <sub>12</sub> coaxial nanocables as ultra high power and long life anode materials for lithium ion batteries. Journal of Materials Chemistry A, 2016, 4, 2089-2095.	10.3	41
117	Facile synthesis of two-dimensional (2D) nanoporous NiO nanosheets from metal–organic frameworks with superior capacitive properties. New Journal of Chemistry, 2016, 40, 1100-1103.	2.8	28
118	Self-Assembled Sandwich-like Vanadium Oxide/Graphene Mesoporous Composite as High-Capacity Anode Material for Lithium Ion Batteries. Inorganic Chemistry, 2015, 54, 11799-11806.	4.0	52
119	Photochromism and fluorescence modulation of pyrazolone derivatives in the solid state. New Journal of Chemistry, 2015, 39, 3059-3064.	2.8	7
120	Facile synthesis of CdS nanorods with enhanced photocatalytic activity. Ceramics International, 2015, 41, 14604-14609.	4.8	31
121	Synthesis, photoisomerization properties and thermal bleaching kinetics of pyrazolones containing 3-cyanobenzal. Spectrochimica Acta - Part A: Molecular and Biomolecular Spectroscopy, 2015, 148, 318-323.	3.9	7
122	Tuning the Color Emission of Sr <sub>2</sub> P <sub>2</sub> O <sub>7</sub> : Tb <sup>3+</sup> , Eu <sup>3+</sup> Phosphors Based on Energy Transfer. Journal of the American Ceramic Society, 2015, 98, 1536-1541.	3.8	51
123	Photoluminescence properties and energy transfer of color tunable MgZn <sub>2</sub> (PO <sub>4</sub> ) <sub>2</sub> :Ce <sup>3+</sup> ,Tb <sup>3+</sup> phosphors. Physical Chemistry Chemical Physics, 2015, 17, 28802-28808.	2.8	23
124	Coal derived porous carbon fibers with tunable internal channels for flexible electrodes and organic matter absorption. Journal of Materials Chemistry A, 2015, 3, 21178-21184.	10.3	70
125	Luminescence properties and energy transfer investigations of Zn2P2O7: Ce3+, Tb3+ phosphor. Journal of Luminescence, 2015, 158, 125-129.	3.1	40
126	Preparation and electrochemical properties of high-capacity LiFePO4–Li3V2(PO4)3/C composite for lithium-ion batteries. Journal of Power Sources, 2014, 246, 912-917.	7.8	39

#	Article	IF	CITATIONS
127	Homogeneous Pd nanoparticles produced in direct reactions: green synthesis, formation mechanism and catalysis properties. Journal of Materials Chemistry A, 2014, 2, 1369-1374.	10.3	61
128	The glucose-assisted synthesis of a graphene nanosheet–NiO composite for high-performance supercapacitors. New Journal of Chemistry, 2014, 38, 2320.	2.8	56
129	A general strategy for synthesis of metal nanoparticles by a solid-state redox route under ambient conditions. Journal of Materials Chemistry A, 2014, 2, 3761.	10.3	43
130	High-yield bamboo-like porous carbon nanotubes with high-rate capability as anodes for lithium-ion batteries. RSC Advances, 2014, 4, 44852-44857.	3.6	34
131	Coal based activated carbon nanofibers prepared by electrospinning. Journal of Materials Chemistry A, 2014, 2, 9338-9344.	10.3	122
132	Hydrothermal synthesis of nitrogen-doped graphene hydrogels using amino acids with different acidities as doping agents. Journal of Materials Chemistry A, 2014, 2, 8352-8361.	10.3	141
133	Enhanced performances of nonenzymatic glucose sensors by attaching Au nanoparticles onto the surfaces of Cu <sub>2</sub> O@Cu nanocable arrays. RSC Advances, 2014, 4, 43973-43976.	3.6	13
134	Solid-state synthesis of SnO <sub>2</sub> –graphene nanocomposite for photocatalysis and formaldehyde gas sensing. RSC Advances, 2014, 4, 46179-46186.	3.6	43
135	One-pot synthesis of Fe3O4/C nanocomposites by PEG-assisted co-precipitation as anode materials for high-rate lithium-ion batteries. Journal of Nanoparticle Research, 2014, 16, 1.	1.9	17
136	Engineering the metathesis and oxidation-reduction reaction in solid state at room temperature for nanosynthesis. Scientific Reports, 2014, 4, 4153.	3.3	18
137	Multimodal porous CNT@TiO2 nanocables with superior performance in lithium-ion batteries. Journal of Materials Chemistry A, 2013, 1, 8525.	10.3	59
138	Effects of Sr-doping on the electrical properties of MnCoNiO4 NTC ceramics. Journal of Materials Science: Materials in Electronics, 2013, 24, 622-627.	2.2	7
139	Preparation and electrochemical properties of LiFePO4/C nanoparticles using different organic carbon sources. Journal of Nanoparticle Research, 2013, 15, 1.	1.9	7
140	Enhanced rate performance of cobalt oxide/nitrogen doped graphene composite for lithium ion batteries. RSC Advances, 2013, 3, 5003.	3.6	44
141	Effective microwave-assisted synthesis of graphenenanosheets/NiO composite for high-performance supercapacitors. New Journal of Chemistry, 2013, 37, 439-443.	2.8	34
142	Synthesis, photochromic properties and thermal bleaching kinetics of pyrazolone phenylsemicarbazones containing a thiophene ring. New Journal of Chemistry, 2013, 37, 2351.	2.8	4
143	Nanoarchitectures constructed with single crystalline Co3O4 spheres and MWCNTs: Temperature effect on the growth and supercapacitors. Materials Research Society Symposia Proceedings, 2013, 1497, 1.	0.1	1
144	THEORETICAL STUDIES ON THE CONFORMATION AND COORDINATION OF N-(1-PHENYL-3-METHYL-4-PROPENYLIDENE-5-PYRAZOLONE)-SALICYLIDENE. Journal of Theoretical and Computational Chemistry, 2013, 12, 1350036.	1.8	0

#	Article	IF	CITATIONS
145	Plum-like and octahedral Co3O4 single crystals on and around carbon nanotubes: large scale synthesis and formation mechanism. RSC Advances, 2012, 2, 3496.	3.6	23
146	Preparation and electrochemical performance of LiFePO4â <sup>~</sup> 'x F x /C nanorods by room-temperature solid-state reaction and microwave heating. Journal of Nanoparticle Research, 2012, 14, 1.	1.9	7
147	Synthesis and electrochemical properties of spinel Li4Ti5O12â <sup>~</sup> 'x Cl x anode materials for lithium-ion batteries. Journal of Solid State Electrochemistry, 2012, 16, 2011-2016.	2.5	39
148	Preparation and characterization of spinel Li4Ti5O12 nanoparticles anode materials for lithium ion battery. Journal of Nanoparticle Research, 2012, 14, 1.	1.9	13
149	Preparation and characterization of high-rate and long-cycle LiFePO4/C nanocomposite as cathode material for lithium-ion battery. Journal of Solid State Electrochemistry, 2012, 16, 17-24.	2.5	23
150	Solid-state photochromism of pyrazolones with highly improved sensitivity, fatigue resistance and reversible fluorescent switching properties. Journal of Materials Chemistry, 2011, 21, 3210.	6.7	27
151	Photochromism and mechanism of pyrazolones in crystals: structural variations directly observed by X-ray diffraction. Journal of Materials Chemistry, 2011, 21, 12202.	6.7	17
152	Graphene–V2O5Â∙nH2O xerogel composite cathodes for lithium ion batteries. RSC Advances, 2011, 1, 690.	3.6	84
153	Synthesis, Crystal Structures and Fluorescent Properties of Two Bimetallic Coordination Polymers. Journal of Inorganic and Organometallic Polymers and Materials, 2011, 21, 254-260.	3.7	2
154	Preparation and characterization of Ag/C nanocables-modified nanosized C-LiFePO4. Journal of Nanoparticle Research, 2011, 13, 4815-4820.	1.9	6
155	Preparation and performance comparison of LiMn2O3.95Br0.05 and LiMn2O3.95Br0.05/SiO2 cathode materials for lithium-ion battery. Journal of Solid State Electrochemistry, 2011, 15, 725-730.	2.5	10
156	Electrochemical deposition of Ni(OH)2/CNTs electrode as electrochemical capacitors. Rare Metals, 2011, 30, 85-89.	7.1	15
157	New insight into the photochromic mechanism of 1,3â€diphenylâ€4â€(4â€fluoro)benzalâ€5â€pyrazolone <i>N</i> (4)â€phenyl semicarbazone. International Journal of Quantum Chemistry, 2011, 111, 1048-1054.	2.0	2
158	Theoretical analysis on the hydrogen bonding and reactivity that associated with the proton transfer reaction of carboxylic acid dimers and their monosulfur derivatives. International Journal of Quantum Chemistry, 2011, 111, 3017-3023.	2.0	3
159	Brâ€Doped Li <sub>4</sub> Ti <sub>5</sub> O <sub>12</sub> and Composite TiO <sub>2</sub> Anodes for Liâ€ion Batteries: Synchrotron Xâ€Ray and in situ Neutron Diffraction Studies. Advanced Functional Materials, 2011, 21, 3990-3997.	14.9	157
160	Synthesis and electrochemical properties of nanosized carbon-coated Li1â^'3x La x FePO4 composites. Journal of Solid State Electrochemistry, 2010, 14, 889-895.	2.5	18
161	Theoretical studies on geometry, solvent effect, and photochromic mechanism of two bisâ€heterocyclic compounds containing pyrazolone ring. International Journal of Quantum Chemistry, 2010, 110, 1360-1367.	2.0	2
162	Simple Solid‣tate Chemical Synthesis of ZnSnO <sub>3</sub> Nanocubes and Their Application as Gas Sensors. European Journal of Inorganic Chemistry, 2009, 2009, 4105-4109.	2.0	57

#	Article	IF	CITATIONS
163	Structure and solid-state photochromic properties of two new compounds with pyrazolone-ring. Structural Chemistry, 2009, 20, 393-398.	2.0	5
164	Conformation and coordination of 1â€phenylâ€3â€methylâ€4â€benzalâ€5â€pyrazolone thiosemicarbazone: A de functional study. International Journal of Quantum Chemistry, 2009, 109, 1341-1347.	ensity 2.0	4
165	Photo-switch and INHIBIT logic gate based on two pyrazolone thiosemicarbazone derivatives. New Journal of Chemistry, 2009, 33, 2232.	2.8	21
166	Three novel photoisomeric compounds of the 4-acyl pyrazolone derivants: Crystal structures and substituent effects on photo-isomerism in solid state. Science in China Series B: Chemistry, 2008, 51, 661-668.	0.8	6
167	Preparation of cobalt and nickel complexes of 8-hydroxyquinoline with nanobelt structure <i>via</i> one-step, low-heating, solid-state reactions. Journal of Coordination Chemistry, 2008, 61, 1019-1026.	2.2	13
168	Crystal structure and photoisomerism of 1-phenyl-3-methyl-4-benzal-5-pyrazolone 4-butylthiosemicarbazone in solid state. Structural Chemistry, 2007, 18, 59-63.	2.0	9
169	Syntheses, crystal structures and thermal behavior of three Mn(II) complexes with 4-acyl pyrazolone derivatives. Structural Chemistry, 2007, 18, 909-915.	2.0	7
170	Preparation and characterization of LiMn2O4 and LiCo0.16Mn1.84O4 as cathode materials for lithium-ion batteries by low heating solid state coordination method. Journal of Materials Science, 2006, 41, 4163-4167.	3.7	3
171	Synthesis and electrochemical performance of LiCr x Mn2-xO4(x=0,0.02,0.05,0.08,0.10) powders by ultrasonic coprecipitation. Journal of Solid State Electrochemistry, 2006, 10, 929-933.	2.5	17
172	Synthesis oftrans-bis(glycinato) copper(II) complex nanorods by room temperature solid-state reaction. Science Bulletin, 2005, 50, 758-760.	1.7	3
173	Synthesis, Structure and Photochromic Properties of 1-Phenyl-3-Methyl-4-(4-Bromobenzal)-Pyrazolone-5 Thiosemicarbazone. Structural Chemistry, 2005, 16, 135-140.	2.0	6
174	Synthesis and Characterization of Tetra-μ-phenolatotetrazinc(II) Complex with 1-Phenyl-3-Methyl-4-(salicylidene hydrazone)-Phenylethylene-Pyrazolone-5. Structural Chemistry, 2005, 16, 431-437.	2.0	22
175	The crystal structure of 1-phenyl-3-methyl-4(salicylaldehyde hydrazone)-propenylidene-5-pyrazolone. Journal of Chemical Crystallography, 2005, 35, 497-501.	1.1	13
176	Synthesis of Metal Complexes of 1â€Phenylâ€3â€methylâ€4â€benzoylpyrazoleâ€5â€one Semicarbazone by Solic and Solution Reactions. Synthesis and Reactivity in Inorganic, Metal Organic, and Nano Metal Chemistry, 2005, 35, 269-274.	lâ€ <b>S</b> tate 0.6	5
177	Synthesis and Crystal Structure of Mixed-Ligand Ni(II) Complex of N-(1-Phenyl-3-methyl-4-benzylidene-5-pyrazolone) p-Nitrobezoylhydrazide and Pyridine. Structural Chemistry, 2004, 15, 327-331.	2.0	23
178	Preparation and characterization of LiMn2O4 nanorod by low heating solid state coordination method. Journal of Nanoparticle Research, 2004, 6, 533-538.	1.9	14
179	SYNTHESIS AND CHARACTERIZATION OF METAL COMPLEXES OF N-(1-PHENYL-3-METHYL-4-BENZAL-5-PYRAZOLONE)-p-METHOXY-BENZOYLHYDRAZINE. Synthesis and Reactivity in Inorganic, Metal Organic, and Nano Metal Chemistry, 2002, 32, 739-751.	1.8	22

1.1 12

#	Article	IF	CITATIONS
181	Synthesis and crystal structure of Schiff base transition metal complex [Co(PMBP-smdtc)2]â‹2H2O. Journal of Chemical Crystallography, 2002, 32, 505-509.	1.1	9
182	Synthesis of CuO nanometer powder by one step solid state reaction at room temperature. Science Bulletin, 1998, 43, 571-573.	1.7	51
183	A Novel Porous N- and S-Self-Doped Carbon Derived from Chinese Rice Wine Lees as High-Performance Electrode Materials in a Supercapacitor. ACS Sustainable Chemistry and Engineering, 0, , .	6.7	17